

See discussions, stats, and author profiles for this publication at: <https://www.researchgate.net/publication/4078353>

Molybdenum-doped indium oxide deposited by radio-frequency magnetron sputtering and pulsed laser deposition

Conference Paper · June 2003

DOI: 10.1109/WCPEC.2003.1305213 · Source: IEEE Xplore

CITATIONS

2

READS

40

8 authors, including:



Timothy Gessert

University of Illinois at Chicago

266 PUBLICATIONS 5,374 CITATIONS

[SEE PROFILE](#)



Der-Liang Young

National Taiwan University

260 PUBLICATIONS 6,644 CITATIONS

[SEE PROFILE](#)



David M. Wood

Colorado School of Mines

39 PUBLICATIONS 2,479 CITATIONS

[SEE PROFILE](#)



John Perkins

National Renewable Energy Laboratory

176 PUBLICATIONS 4,739 CITATIONS

[SEE PROFILE](#)

MOLYBDENUM-DOPED INDIUM OXIDE DEPOSITED BY RADIO-FREQUENCY MAGNETRON SPUTTERING AND PULSED LASER DEPOSITION

Y. Yoshida,¹ C. Warmsingh,¹ T. A. Gessert,² D. L. Young,² D. M. Wood,¹ J. D. Perkins,² D. S. Ginley,² and T. J. Coutts²

¹Colorado School of Mines, 1500 Illinois St. Golden, CO 80401 USA

²National Renewable Energy Laboratory (NREL), 1617 Cole Blvd., Golden, CO 80401 USA

ABSTRACT

Thin-films of molybdenum-doped indium oxide (IMO), an n-type transparent conducting oxide, were deposited using radio-frequency (RF) magnetron sputtering and pulsed laser deposition (PLD). To date, sputtered and PLD IMO films have exhibited mobilities as high as 45 and 127 cm²V⁻¹s⁻¹. Temperature-dependent Hall measurements were done on both sputtered and PLD films to study scattering mechanisms. In addition, four transport coefficient measurements (conductivity, Hall, Nerst, and Seebeck coefficients) were conducted to extract the transport properties of IMO. Temperature-dependent Hall measurements on PLD and sputtered films suggest the mobility is limited by phonon and ionized impurity scattering, respectively. From the method of four coefficients, the density-of-states effective-mass value of IMO was found to increase from ~0.25m_e to ~0.4m_e as carrier concentration varied from 3.6×10¹⁹ to 6.5×10²⁰ cm⁻³.

1. INTRODUCTION

Transparent conducting oxides (TCOs) have played a vital role in flat-panel displays, low-emissivity windows, and solar cells [1] because of their desirable optical and electrical properties. Because demands for electrical conductivity and optical transparency continue to increase, new TCO materials with properties more appropriate for specific applications continue to be sought. In general, the properties required for a useful TCO material are a resistivity on the order of <10⁻² Ωcm and a visible transmittance of >80%. Further, for many future applications, it is preferred that low resistivity be attained through high electron mobility, rather than high carrier concentration [2]. High mobility and/or high carrier concentration can lead to high conductivity. However, high mobility will not only increase conductivity, but will also minimize absorptance in the near-infrared (NIR) spectral region. In contrast, high carrier concentration increases NIR absorption through a shift in the plasma edge.

Several TCO materials, such as SnO₂:F and ZnO:Al are available commercially; however, In₂O₃:Sn (ITO) is often preferred due to its high optical and electrical quality. Although ITO has been used extensively for almost 40 years, fundamental limitations on electrical transport in the material and the band structure remain poorly understood.

Band diagrams for In₂O₃ and ITO proposed in 1977 by Fan and Goodenough [3] are often used to explain its high optical transparency. More recently, Mryasov and Freeman [4] have computed the band structure of In₂O₃ and ITO. Together, these studies suggest that significant questions remain regarding the fundamental material properties of

In₂O₃. Unambiguous identification of the dominant charge scattering mechanism(s) in In₂O₃ and ITO has not been demonstrated to date, because values of effective mass, dielectric permittivity, etc., have been unavailable [5]. In contrast, the method of four coefficients provides much more direct information regarding which scattering mechanisms are limiting mobility.

The method of four coefficients was originally developed by Kaydanov and coworkers in the 1960s [6]. The original apparatus was built to measure the conductivity, Hall, Nerst, and Seebeck coefficients for bulk materials. An apparatus was constructed at NREL by Mulligan [7] and later modified and improved by Young [8]. These were designed to allow measurement of transport coefficients for both thin films and bulk materials. These four transport coefficients can be used with solutions to the Boltzmann transport equation to extract the carrier density-of-states (DOS) effective mass, the Fermi level relative to the conduction-band minimum, and an energy-dependent scattering parameter that is related to a relaxation time. Mulligan studied cadmium stannate (CTO), treating the conduction band as parabolic. Later, Young corrected for the measured band non-parabolicity on a new set of CTO data. This non-parabolicity correction affected the values of the scattering parameter and the Fermi level of CTO, and resulted in identifying the dominant scattering mechanism in CTO as optical phonon-like scattering.

Young [9] also measured coefficients of amorphous and polycrystalline zinc stannate (ZTO). In ZTO, non-parabolicity of the conduction band was again observed. He determined that the effective mass of ZTO increases with carrier concentration from 0.16 to 0.26 m_e as the Fermi energy increased from 0.09 to 0.2 eV. Ionized impurity scattering, modified by screening from free electrons for highly degenerate films, was observed.

Another method that can identify scattering mechanisms is temperature-dependent Hall measurements. Scattering rates predicted from Fermi Golden Rule calculations have distinct temperature dependences that depend on specific scattering mechanisms [10].

In this study, we investigate a relatively new TCO, molybdenum-doped indium oxide (IMO). This study was prompted by reported mobilities of 80 – 130 cm²V⁻¹s⁻¹ for thermally evaporated IMO films [11,12]. These are among the best electrical properties for doped indium oxide ever reported. To expand our understanding of scattering mechanisms and the band structure of IMO, along with an effort to find a method to achieve better quality films, the present study uses radio-frequency (RF) sputtering and pulsed laser deposition (PLD) systems and uses temperature-dependent Hall and the method of four coefficients to probe the band structure.

2. EXPERIMENTAL SETUP

Films were prepared using RF magnetron sputtering at 13.56 MHz in a sputter-down configuration from 2-inch diameter planar targets of 99.99% purity. All IMO targets were hot pressed using fully oxidized In_2O_3 . The targets were purchased from Cerac, Inc. (Milwaukee, WI). The composition of the IMO target used for sputtering was 96 wt.% In_2O_3 and 4 wt.% Mo metal. For PLD films, targets were made with molybdenum contents of 1, 2, and 4 wt%. Sputter deposition was performed in a Unifilm sputtering system capable of automated control of both substrate orbit and rotary motion to enhance deposit uniformity. Base pressures of 5×10^{-8} – 2×10^{-7} torr were established using a cryopump prior to each deposition. Ultra-high-purity oxygen (99.993% purity) and/or argon (99.999% purity) were used as the sputtering gases, and the partial pressures were set using needle valves prior to throttling to the sputtering pressure of 10 mtorr. Sputtering was conducted in constant power mode at 80 W.

For sputtered films, Corning 7059 glass substrates were cleaned using a 5% solution of 18 Mohm deionized water and Citranox in an ultrasonic bath for 10 minutes, followed by rinsing in deionized water, spin rinsing to an output water resistivity of 12 Mohm, and spin drying. Substrates were placed on a rotatable heater (boron-nitride element) operating at a constant voltage. Depositions were performed at substrate temperatures of 120°–420°C. The substrate temperature was calibrated by placing a 0.32-cm-thick Al block with an embedded thermocouple at the substrate position, and allowing the block to equilibrate for 2 hours. The source-substrate separation was ~1.27 cm. Following deposition, the samples were maintained in the sputtering ambient and temperature for one hour, after which the gases and heater were shut off, and the substrate was allowed to cool under vacuum for 1 hour. This post-deposition procedure was critical for both high-mobility samples and reproducibility of film electrical parameters.

The PLD chamber consists of a 12-inch spherical cross with a Neocera 6 target carousel configured with a 2-inch-diameter resistance heater. The chamber was evacuated to a base pressure in the range of $\sim 10^{-7}$ torr, using a turbo pump prior to deposition, and was then backfilled with pure oxygen to the total pressure of 2 mtorr. The target-to-substrate distance was fixed at 8.5 cm. The target carousel was rotated and rastered under computer control so that the beam ablated the face of the target more uniformly than a simple racetrack pattern, which would result from rotation alone. The ablating laser was a Lambda Physik EMG 103 excimer laser (KrF 248 nm) with laser power of 300 mJ/pulse. Typical films were deposited with ~35,000 pulses. Substrate temperature, pulse rate, and atmosphere were controlled during growth runs. The films were deposited at a total pressure of 2 mtorr in an oxygen atmosphere and at a substrate temperature of 350°C. As-

received Corning 1737 glass and (100) single-crystal yttria-stabilized zirconia (YSZ) substrates were used for PLD films. One sputtered film with high carrier concentration was subsequently annealed repeatedly for ~3-hour intervals at 400°C in oxygen and the properties were measured after each anneal.

The thickness of the ~0.2–1- μm -thick films was measured using stylus profilometry (Veeco Dektak 3), and the 0.01–0.2- μm -thick films were measured using ellipsometry (Rudolph Research Type 43702-200E). The film resistivity, mobility, and carrier concentration were obtained at room temperature from Hall analysis using the van der Pauw method (BioRad HL5500 System). In addition, temperature-dependent Hall measurements were carried out over a temperature range of 105K to 370K. The four-coefficient measurement system assembled by Young [13] was used to measure transport properties of the films. XRD measurements were made using Cu $K\alpha$ radiation (Scintag DMS2000).

3. RESULTS AND DISCUSSION

To date, the highest mobility observed for sputtered film on Corning 7059 glass substrate is $45 \text{ cm}^2\text{V}^{-1}\text{s}^{-1}$ with a carrier concentration of $1.8 \times 10^{20} \text{ cm}^{-3}$. This was produced in a low oxygen concentration environment and at a substrate temperature of ~400°C [14]. Because sputtered films have shown potential, PLD (which often yields high quality material) studies were initiated using targets with 1, 2, and 4 wt% Mo content on both single-crystal YSZ (100) and Corning 1737 glass substrates. Films with 2 wt% molybdenum content produced the highest mobility, compared to 1 and 4 wt% films, on both YSZ and glass substrates [15]. The highest mobilities achieved for PLD films with 2 wt% Mo on glass and on YSZ were 111 and $127 \text{ cm}^2\text{V}^{-1}\text{s}^{-1}$ with carrier concentrations of 1.7×10^{20} and $1.9 \times 10^{20} \text{ cm}^{-3}$, respectively. For 4 wt% Mo film on glass and YSZ, mobilities were 43 and $54 \text{ cm}^2\text{V}^{-1}\text{s}^{-1}$, respectively. Note that the mobilities of 4 wt% Mo PLD and sputtered films on glass are very similar.

Sputtering on YSZ was attempted using the optimum conditions described above, but micro-cracking between terraces observed by scanning electron microscopy (shown in Figure 1) made the film highly resistive, even though the films were confirmed to be epitaxial by X-ray pole figure. Figure 2 shows XRD patterns for 4 wt% Mo sputtered films on glass and YSZ and for 2 wt% Mo PLD films on glass and YSZ. Although both sputtered and PLD films on glass are randomly oriented, films on YSZ are epitaxial. We suggest that the preferred orientation of the film on YSZ may be linked to better electrical properties, as seen in the PLD result.

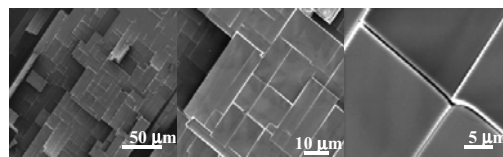


Figure 1. SEM image of sputtered film on YSZ (100).

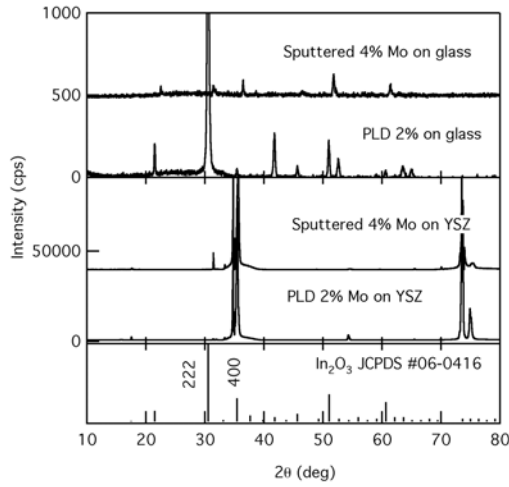


Figure 2. XRD image of sputtered and PLD films on glass and YSZ (100).

Temperature-dependent Hall measurements were conducted on 4 wt% Mo sputtered films on glass and 4 and 2 wt% Mo PLD films on glass and YSZ to see if we could identify the difference in scattering mechanisms of differently doped films on different kinds of substrates deposited by different methods, as shown in Figure 3. The data denoted "A" are annealed samples with carrier concentrations between 2×10^{20} and $5 \times 10^{20} \text{ cm}^{-3}$, which cannot be achieved by controlling oxygen partial pressure during deposition. There are three significant points that should be noted from this figure. First, 4 wt% Mo sputtered films with high carrier concentrations demonstrated that the carrier concentration varies strongly with temperature, even though the mobility remains relatively constant. This

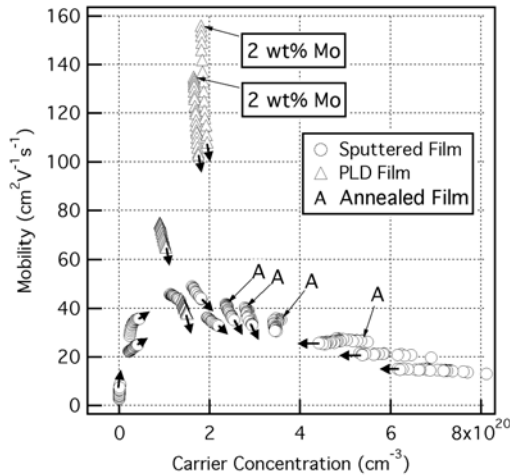


Figure 3. Temperature dependent analysis of sputtered and PLD IMO films. All films are produced from 4 wt% Mo targets, except where indicated. Arrow indicates the direction of increase in temperature.

contrasts with 2 wt% Mo PLD films, where the mobility varies significantly as the temperature is varied but the carrier concentration remains relatively constant with temperature. Second, the carrier concentration decreased as temperature increased at higher carrier concentrations, but this trend reversed at $\sim 3.5 \times 10^{20} \text{ cm}^{-3}$. At the same point, the temperature dependence of the mobility changes as well. At high carrier concentrations, the mobility was constant with temperature, but began to decrease with temperature at carrier concentrations lower than $3 \times 10^{20} \text{ cm}^{-3}$. Finally, temperature dependence of the mobility is different at lower carrier concentrations ($\sim 3 \times 10^{19} \text{ cm}^{-3}$), where an increase in mobility with temperature is observed.

From mobility data over this temperature range, phonon scattering and ionized impurity scattering are suggested for high-mobility PLD and high-carrier-concentration sputtered films, respectively, because mobility changed strongly with temperature for the first and remained constant for the latter sample. Results for the PLD film seem to coincide with the data for CTO [2], which is considered one of the best TCO materials available in terms of optical and electrical properties. Young et al. found that CTO exhibited optical phonon scattering as its dominant scattering mechanism. Our PLD IMO films with 2 wt% Mo on YSZ and glass are among the best ever reported. This phonon scattering may indicate that further increases in mobility could be challenging due to the intrinsic nature of phonons. These data also suggests that 2 wt% could be the solubility limit of molybdenum in In_2O_3 . The carrier concentration did not change significantly between films with 1, 2, and 4 wt% Mo, but the mobility was highest at 2 wt% and decreased when it was doped with 4 wt% Mo [15]. It is possible that excess Mo could cause defects that could lower mobility in the case of 4 wt% Mo films.

In addition to temperature-dependent Hall measurements, the method of four coefficients was applied to all the sputtered films to understand the shape of the conduction band, the DOS effective mass variation with Fermi energy, and the scattering mechanism. The DOS

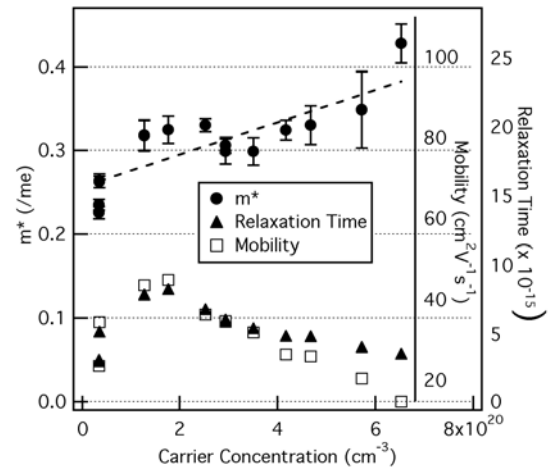


Figure 4. Results from four-coefficient measurement.

effective mass is shown in Fig. 4. At first glance, one observes that the effective mass increases from $0.25m_e$ to $0.4m_e$ as the carrier concentration increases from 3.6×10^{19} to $6.5 \times 10^{20} \text{ cm}^{-3}$, which clearly indicates non-parabolicity of the conduction band. This non-parabolicity was observed for previously studied CTO and ZTO as well [2,16]. The slope of this graph allows us to calculate a non-parabolicity correction, which enables us to calculate the scattering parameter, the Fermi level with respect to the conduction-band minimum [17]; the estimated slope for our data is shown in Fig. 4. At this stage, the correction term cannot be determined with confidence due to scatter of the data. Therefore, the dominant scattering mechanism and Fermi energy of IMO have not yet been identified from the data.

4. CONCLUSION

IMO films were deposited by RF magnetron sputtering and PLD. All the films were tested with temperature-dependent Hall and four-coefficient measurements. We found that high-mobility PLD films with 2 wt% Mo content showed phonon scattering, and the high-carrier-concentration sputtered film with 4 wt% Mo showed ionized impurity scattering. In addition, the data indicate that there is a point where the scattering mechanism changes around $3 \times 10^{20} \text{ cm}^{-3}$ because mobility and carrier-concentration dependence on temperature change significantly. From four-coefficient measurements, we found that the DOS effective mass changed from $0.25m_e$ to $0.4m_e$ as carrier concentration increased from 3.6×10^{19} to $6.5 \times 10^{20} \text{ cm}^{-3}$. This confirmed the non-parabolicity of the conduction band.

7. ACKNOWLEDGEMENT

The authors would like to thank Dr. V. Kaydanov for discussion. This work was supported by the U.S. Department of Energy under Contract no. DE-AC36-99GO10337.

REFERENCES

- [1] R. G. Gordon, *MRS Bulletin* **25**, 52 (2000).
- [2] T. J. Coutts, D. L. Young, and X. Li, *MRS Bulletin* **25**, 58 (2000).
- [3] J. C. C. Fan and J. B. Goodenough, *J. Appl. Phys.* **48**, 3524 (1977).
- [4] O. N. Mryasov and A. J. Freeman, *Phys. Rev. B* **64**, 233111 (2001).
- [5] T. J. Coutts, T.A. Gessert, R.G. Dhere, A.J. Nelson, and H. Aharoni, *Rev. Brasil. Appl. Vac.* **6**, 289 (1986).
- [6] V. I. Kaydanov and I. S. Lisker, *Zavodskaya Laboratoriya* **32**, 1091 (1966).
- [7] W. P. Mulligan, "A Study of the Fundamental Limits to Electron Mobility in Cadmium Stannate Thin Films" (Ph.D. Thesis, Colorado School of Mines, 1997).
- [8] D. L. Young, "Electron Transport in Zinc Stannate (Zn_2SnO_4) Thin-Films" (Ph.D. Thesis, Colorado School of Mines, 2000).
- [9] D. L. Young, T. J. Coutts, B. I. Kaydanov, A. S. Gilmore, and W. P. Mulligan, *J. Vac. Sci. Technol. A* **18**, 2978 (2000).
- [10] B. M. Askerov, *Electron Transport Phenomena in Semiconductors*, World Scientific Publishing:River Edge, NJ, 1994.
- [11] Y. Meng, X. Yang, H. Chen, J. Shen, Y. Jiang, Z. Zhang, and Z. Hua, *Thin Solid Films* **394**, 219 (2001).
- [12] Y. Meng, X. Yang, H. Chen, J. Shen, Y. Jiang, Z. Zhang, and Z. Hua, *J. Vac. Sci. Technol. A* **20**, 288 (2002).
- [13] D. L. Young, T. J. Coutts, B. I. Kaydanov, A. S. Gilmore, and W. P. Mulligan, *J. Vac. Sci. Technol. A* **18**, 2978 (2000).
- [14] Y. Yoshida, T. Gessert, C. Perkins, and T. Coutts, *J. Vac. Sci. Technol. A* (2003) in press.
- [15] C. Warm Singh, Y. Yoshida, D. Readey, J. Perkins, P. Parilla, C. Teplin, T. Kaydanova, J. Alleman, L. Gedvilas, B. Keyes, T. Gessert, T. Coutts, and D. Ginley, *Proceedings of NREL NCPV Review Meeting*, Denver, CO 2003.
- [16] D. L. Young, D. L. Williamson and T. J. Coutts, *J. Appl. Phys.* **91**, 1464 (2002).
- [17] D. L. Young, "Electron Transport in Zinc Stannate (Zn_2SnO_4)" (Ph.D. Thesis, Colorado School of Mines, 2000).